

# Experimental Observation and Numerical Prediction of Induction Heating in a Graphite Test Article

Todd A. Jankowski\*<sup>1</sup>, Debra P. Johnson<sup>1</sup>, James D. Jurney,<sup>1</sup> Jerry E. Freer,<sup>1</sup> Lisa M. Dougherty,<sup>1</sup> and Stephen A. Stout<sup>1</sup>

<sup>1</sup>Los Alamos National Laboratory, Los Alamos, NM 87545, USA

\*Corresponding author: MS J580, Los Alamos, NM 87545; jankowski@lanl.gov

**Abstract:** The induction heating coils used in the plutonium casting furnaces at the Los Alamos National Laboratory are studied here. A cylindrical graphite test article has been built, instrumented with thermocouples, and heated in the induction coil that is normally used to pre-heat the molds during casting operations. Preliminary results of experiments aimed at understanding the induction heating process in the mold portion of the furnaces are reported. The experiments have been modeled in COMSOL Multiphysics and the numerical and experimental results are compared to one another. These comparisons provide insight into the heating process and provide a benchmark for COMSOL calculations of induction heating in the mold portion of the plutonium casting furnaces.

**Keywords:** Induction heating, metal casting.

## 1. Introduction

The plutonium casting furnaces at the Los Alamos National Laboratory use two separate induction heating coils. One induction coil is used to melt plutonium in a tantalum crucible. The other coil is used to pre-heat a graphite mold. Molten plutonium is then poured by gravity from the crucible into the pre-heated mold. A number of upgrades of furnace components are planned to allow for more flexibility in the use of the casting furnaces (e.g., casting over a wide range of temperatures, casting into molds with a variety of geometries, achieving precise control of cooling rates after casting). One critical component of the furnace is the induction coil used to pre-heat the mold. Experiments and numerical modeling are currently being performed to understand the heating process in the mold portion of the casting furnace. Once the modeling capability is validated by comparisons to the experimental results, models will be used to suggest possible design enhancements to the induction coils that

would allow for future flexibility in casting operations.

To better understand the induction heating process in the mold portion of the furnace, a simple cylindrical graphite test article has been built and instrumented with thermocouples. The graphite test article and the induction coil are shown in Fig. 1.

The graphite test article is a hollow cylinder 19.05 cm (7.5 in) in height with a 1.27 cm (0.5 in) thick wall. The end caps of the test article are 2.54 cm (1 in) thick. The test article is made from 2020 grade isostatically pressed graphite. For all of the tests described here, the test article has been instrumented with six thermocouples placed at the locations shown in Fig. 2.

The induction coil used to heat the graphite test article is a 5 turn coil made from 0.635 cm (0.25 in) thick solid copper bar. The coil is wound with a step pattern between turns near the current leads. This pattern is sometimes used in induction coils to reduce the influence of end effects that are present when using helical coils and to provide more uniform volumetric heating.<sup>1</sup> Induction heating is achieved by supplying AC power at 9600 Hz to the coil through the current leads shown in Fig. 1.

The entire casting furnace is enclosed in a vacuum vessel. The outer walls of the vacuum vessel surrounding the mold portion of the furnace are water cooled, allowing the walls of the vacuum vessel to maintain temperatures near room temperature. These walls serve as a constant temperature radiation boundary for the test article and induction coil. Due to safety considerations in the plutonium casting process, water is not allowed in the vacuum enclosure. As a result, the induction coil is not water cooled. The coil is only cooled by radiation to the walls of the vacuum vessel.

In Sec. 2, we present the two and three-dimensional COMSOL models used to study the heating in the mold portion of the furnace. In Sec. 3, we compare results of the models to the experimental data gathered during testing. In

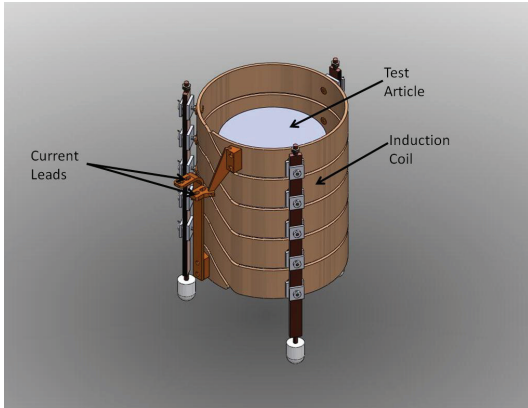


**Figure 1.** The mold coil and the test article.

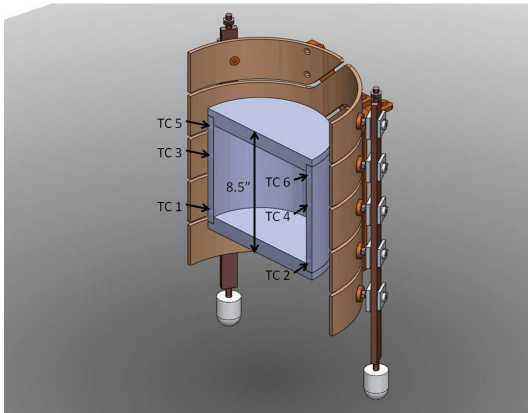


**Figure 2.** The positions of the thermocouples (TC) in the test article.

Sec. 4, we discuss differences between the modeling results and the experimental observations and we give suggestions for future work. Finally, conclusions are given in Sec. 5.

## 2. Use of COMSOL Multiphysics

A simplified version of the induction coil is used for the finite element simulations. The three-dimensional geometry imported into COMSOL is shown in Fig. 3. A two-dimensional axis-symmetric model shown in Fig. 4 was also built in COMSOL. The pre-defined transient analysis, induction heating, electro-thermal interaction mode in the AC/DC module is used for the models. The induction heating simulations use the quasi-static, induction currents, time-harmonic application mode (azimuthal induction currents in 2-D) to solve for the magnetic vector potential. The pre-defined couplings then use the calculated volumetric

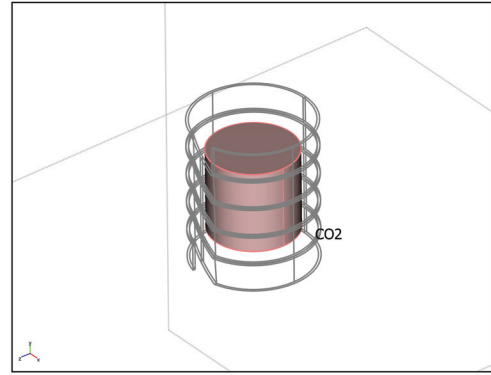


**Figure 3.** The three-dimensional geometry used in the COMSOL simulations.

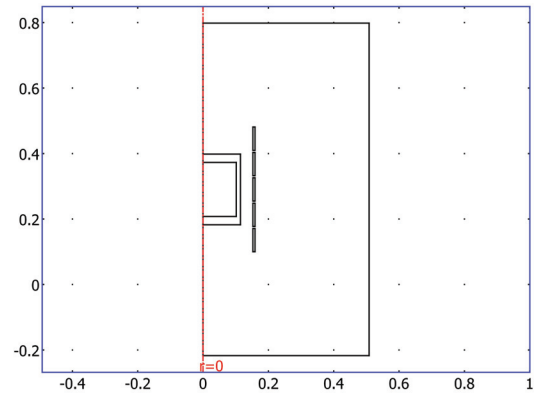


**Figure 4.** The two-dimensional geometry used in the COMSOL simulations.

heating from the induction currents application mode as a source term in the energy equation for a transient heat transfer simulation in the general heat transfer application mode.

A number of assumptions are used in defining the model. First, the current in the induction coil is treated as a surface current boundary condition on the inner surface of the coil. At 9600 Hz, the skin depth in copper is  $\sim 1/10^{\text{th}}$  the thickness of the coil used in the furnace. Secondly, the electrical conductivity of graphite is assumed to be constant over the temperature ranges considered. The maximum temperature of the test article is limited to 600 °C during the experiments. The electrical conductivity of graphite changes by less than 15% between room temperature and 600 °C, so that our assumption of a constant conductivity will lead to only a small error. Finally, the resistive losses in the copper are treated as a boundary condition in the heat transfer

simulation only. The surface heat flux at the inner surface of the induction coil is calculated from

$$\dot{q}'' = \frac{1}{2} \frac{J_s^2}{\sigma_{cu} \delta_{cu}},$$

where  $J_s$  is the surface current density,  $\sigma_{cu}$  is the electrical conductivity of copper, and  $\delta_{cu}$  is the skin depth in the copper.

As a result of these assumptions, the electromagnetic and heat transfer simulations can be de-coupled from each other and solved separately. Furthermore, by not explicitly modeling the copper in the induction currents application mode, and by calculating the resistive heating with the equation above, the electrical conductivity of the copper can be treated as a function of temperature. Additionally, temperature dependent thermal properties (thermal conductivity and specific heat) are used for the graphite and copper in the heat transfer simulations.

Finally, in the heat transfer application mode, all initial temperatures are set to 20 °C. All surfaces on the test article and induction coil are allowed to participate in surface-to-surface or surface-to-ambient radiation. The surface emissivity of the graphite is set to 1, while the surface emissivity of the copper is set to 0.75.

### 3. Experimental and Numerical Results

Experiments with the graphite test article in the induction coils have only recently begun and are on-going. We report on preliminary comparisons between one of the experimental runs and the COMSOL model. In the experiment, the graphite test article was centered axially and concentrically in the induction coil.

The current through the induction coil is automatically controlled by the power supply during warm-up of the graphite test article from ambient conditions. The average of thermocouples 3 and 4 (see Fig. 2) was used as a control point. The set point for the controller was 575 °C. The current supplied to the induction coil, as a function of time, is shown in Fig. 5.

For the comparisons between the experimental and numerical results, we are primarily concerned with the steady-state results. In the finite element simulations, trying to

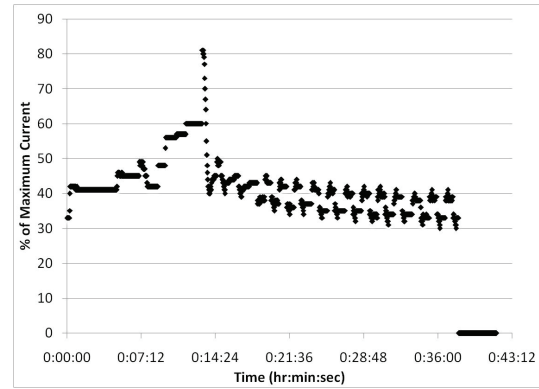


**Figure 5.** Current supplied to the induction coil by the power supply during the experiment.

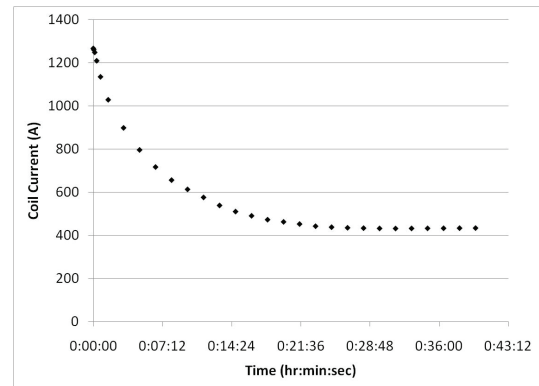


**Figure 6.** Surface current determined by the PID controller and used in the finite-element simulations.

accurately reproduce the temperatures in the test article during the warm-up period, when the current shown in Fig. 5 was applied to the induction coils, would require a large number of time steps to capture the rapid changes in current supplied to the induction coil by the controller. Rather than applying the coil current shown in Fig. 5, we use a simulated PID controller to control the current in the induction coil for the finite-element simulations. The two-dimensional model shown in Fig. 4 was used to determine the current as a function of time using PID control.<sup>2</sup> A set-point temperature of 575 °C was used, and the parameters in the simulated PID controller were determined using the Ziegler-Nichols method.<sup>3</sup> The current determined by the simulated PID controller is shown in Fig. 6. The current determined in the two-dimensional model was used as an input to the three-dimensional simulations.

In Fig. 7, the control point temperature (average of thermocouples 3 and 4) from the

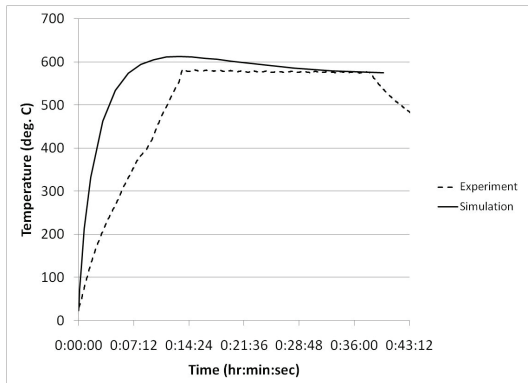


**Figure 7.** The control point temperatures (average of TC3 and TC4) for the experiment and the COMSOL simulation during the warm-up period.

experiments and from the three-dimensional finite-element simulations are compared. Although the simulated PID controller drives the control temperature considerably higher than the temperatures observed in the experiments during the initial portion of the warm-up period, the rise time, settling time, and overshoot for the experiments and the finite-element simulations are comparable.

Figures 8 and 9 show the temperatures in the test article during the last portion of the warm-up as the temperatures come to steady-state. Although there are considerable differences between the experimental and numerical results (these differences will be discussed in the next section), both the experiments and the finite element simulations show that the odd-numbered thermocouples are typically 10 to 15 °C higher in temperature than the even numbered thermocouples at the same axial location in the test article. This non-uniform heating of the molds during casting operations was observed in the past, but the non-uniformity was always attributed to misalignment of the induction coils with respect to the molds and/or vacuum can or to variations in material properties and geometry. The experimental and numerical results presented here with the test article centered in the induction coil, however, show that the magnetic field produced by the induction coil itself is leading to the observed non-uniform temperature distributions.

Figure 10 shows a cross-section plot of the resistive heating in the test article through the locations with thermocouples 3 and 4. The figure shows that the resistive heating on the side of the test article with the odd numbered

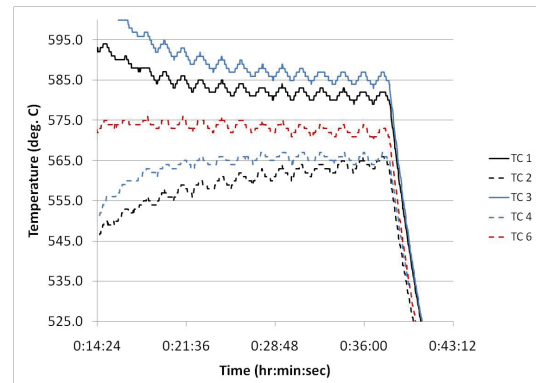


**Figure 8.** Measured (experimental) temperatures in the test article as the system comes to steady-state.

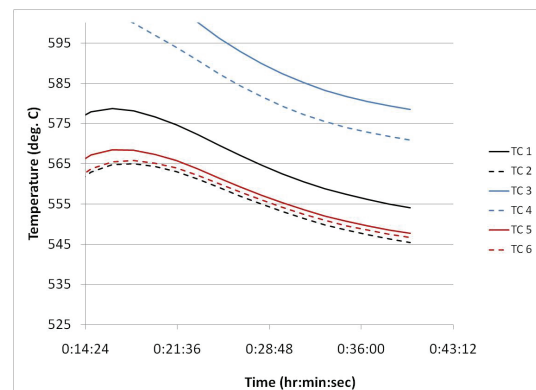


**Figure 9.** Calculated (finite-element simulation) temperatures in the test article as the system comes to steady-state.

thermocouples is 5-10% higher than on the side with the even numbered thermocouples. Referring to Figs. 1 and 2 and viewing the test article from above, the odd numbered thermocouples are 90 degrees counter-clockwise from the step in the induction coil. Careful consideration of the magnetic field produced by the induction coil, and particularly the portion of the induction coil with the step, leads to the expectation of higher flux densities and higher levels of resistive heating in the test article near the odd numbered thermocouples compared to the locations with the even numbered thermocouples.

In Fig. 11, a slice plot showing temperatures through the axial center of the test article is presented. The figure shows that because of the distortion of the magnetic field caused by the step in the induction coil, the side of the mold nearest the step is heated to temperatures 25-30 °C higher than the rest of the mold.

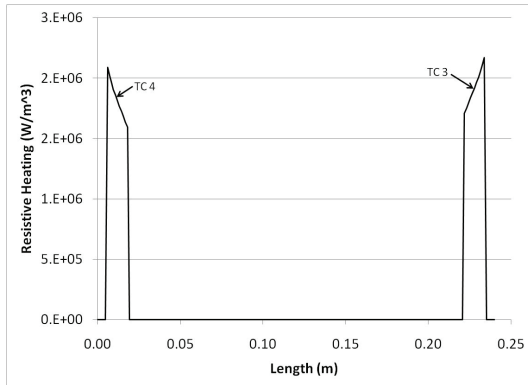


**Figure 10.** Resistive heating in the test article at time 39 min 54 sec as calculated by the finite element simulation. The resistive heating is plotted along a line passing through the locations of TC3 and TC4.

#### 4. Suggestions for Future Work

Although the finite-element simulations do show the non-uniform heating in the test article observed in the experiments, there are significant differences between the calculated and observed temperatures near the end caps of the cylindrical test article (thermocouples 1 and 2 and thermocouples 5 and 6). Comparing Figs. 8 and 9, shows that in the experiments, these thermocouples near the ends of the cylindrical test article are at higher temperatures than the temperatures predicted by the finite element analysis. These discrepancies are likely caused by two factors. First, in the experiments, the test article is supported by a ceramic test stand that likely insulates the bottom of the cylinder. Secondly, in the finite-element analysis, the walls of the vacuum chamber (the radiation boundaries) are assumed to be at a constant temperature of 20 °C throughout the simulations. It is possible that the temperature of these walls may increase throughout the heating process. In future modeling efforts, these effects will be incorporated into the simulations. Additionally, we plan to incorporate a more representative control system for the coil current into the finite element simulations so that the transient behavior of the test article can be calculated and compared to the experimental observations.

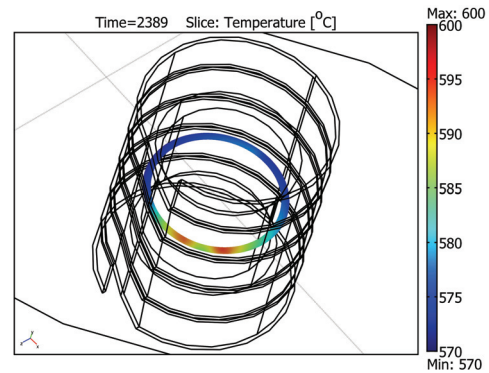


**Figure 11.** Temperature in a slice through the axial center of the cylindrical test article. The temperature distribution shows a region of high temperature near the step in the induction coil.

#### 5. Conclusions

We have developed transient models of the induction heating process in the mold portion of the plutonium casting furnaces at the Los Alamos National Laboratory. A cylindrical graphite test article has been built, instrumented with thermocouples, and placed in the induction coil. Temperature measurements have been compared to calculated temperatures from a three-dimensional COMSOL Multiphysics model. Both the numerical and experimental results show a non-uniform temperature distribution in the test article. After inspection of the finite element results, we attribute the non-uniform temperature distribution to the distortion of the magnetic field caused by the geometry of the induction coil. COMSOL simulations will be used in the future to direct design decisions for the next generation of induction heating coils used in the plutonium casting furnaces and to suggest coil designs that will allow for more flexibility in the use of the casting furnaces.

#### 6. References

1. Zinn, S. and Semiatin, S. L., *Elements of Induction Heating*, pg. 34. EPRI, (1988)
2. COMSOL AB, *COMSOL Multiphysics Model Library*, pp. 317-322. COMSOL 3.4, (2007)
3. Jacob, J. M., *Industrial Control Electronics: Application and Design*, pp. 279-324, (1988)